

# Dependence of particle size distribution upon brittleness in glass

Seongjin Hwang, Hyungsun Kim\*

*School of Materials Engineering, Inha University, 253 Yonghyun-dong, Nam-gu, Incheon 402-751, Republic of Korea*

Received 18 January 2007; received in revised form 23 April 2007; accepted 5 May 2007

Available online 27 July 2007

## Abstract

The size reduction of glasses is dependent on the impact energy and their brittleness. In milling, the particle size distribution is especially related to the glass brittleness, which can be predicted by the experimentally determined elastic modulus. The correlation of glass mechanical properties with particle size distribution during dry milling was investigated. The  $D_{50-90}$  particle size distribution and mean particle size were related to the glass brittleness. We suggest that the relationship between frit size distribution and brittleness should be considered for efficient pulverization, and further that the glass brittleness can be predicted by the elastic modulus of glasses.

© 2007 Elsevier Ltd. All rights reserved.

**Keywords:** Mechanical properties; Fracture; Elastic modulus; Glass; Milling

## 1. Introduction

Glass frits have been used for many applications such as glaze coating, sealing glass, and electric devices, as well as for forming the main components of the flat panel display (FPD), especially plasma display panel (PDP), such as transparent dielectric, barrier rib, sealing material, and electrode.<sup>1–3</sup> Various glass systems such as lead oxide, borate, bismuth, and phosphate have been utilized as glass frits in PDP. Recently, however, the use of lead oxide frits has had to be remarkably reduced in PDP applications because of environmental pollution.<sup>1–3</sup>

Grinding has been one of the most important unit operations in many fields such as chemical, pharmaceutical and material industries.<sup>2–5</sup> Recently, much attention has been paid to fine grinding due to its importance for nano-technology and nano-materials. Comminution is the oldest mechanical unit operation for size reduction of a solid mass used to generate a large quantity of particulate materials. It is well recognized that grinding effects are sensitively dependent on ball motion, especially impact energy, which is influenced by grinding conditions such as the pot diameter, pot depth, ball diameter, ball-filling ratio, revolution radius, rotational speed and grinding materials.<sup>4,5</sup> Moreover, grinding materials have their own individual mechanical properties such as elastic modulus, hardness, brittleness, and

strength. In the case of glasses, the mechanical failure of glasses is especially related to their brittleness.<sup>6</sup>

Generally, wet grinding is a more suitable method than dry milling to obtain finer frit because the ground powder is obtained in a less agglomerated state. However, solvent molecules and contamination are adsorbed on the newly formed surface of the particles in wet milling, which is a significant cause of defects in electric devices.<sup>2–5</sup> Therefore, we studied dry milling with the glasses used in PDP production. The particle size distribution was examined according to the milling condition and the correlation of glass mechanical properties with particle size distribution during dry milling was investigated. The results are discussed to elucidate the relationship between particle size distribution and glass brittleness and to prepare preliminary results for lead-free frit.

## 2. Experimental procedure

The  $\text{PbO-SiO}_2\text{-Al}_2\text{O}_3$  (L) and  $\text{Bi}_2\text{O}_3\text{-B}_2\text{O}_3\text{-ZnO}$  (A and B) glass systems were used for this experiment. The batch compositions, consisting of high purity raw materials (>99.9% Aldrich, USA), were well mixed in ball mills for 12 h for the three glasses and the compositions are presented in Table 1. The batches were melted in an alumina crucible at 1150–1200 °C for 30 min and the melt was quenched into a stainless roller to make a cullet. At the first crushing, the cullet was crushed with a hand mill using an agate (mortar and pestle) and sieved with 140 mesh

\* Corresponding author. Tel.: +82 32 860 7545; fax: +82 32 864 3730.  
E-mail address: [kimhs@inha.ac.kr](mailto:kimhs@inha.ac.kr) (H. Kim).

Table 1  
Composition of the three glasses

Glasses	Composition (mol%)							
	PbO	Bi <sub>2</sub> O <sub>3</sub>	B <sub>2</sub> O <sub>3</sub>	SiO <sub>2</sub>	ZnO	BaO	CeO <sub>2</sub> + TiO <sub>2</sub>	Al <sub>2</sub> O <sub>3</sub>
L	36	–	6	54	–	–	1	3
A	–	11	40	7.8	27	10	0.2	4
B	–	12	33	–	54	–	1	–

(<106 μm) and pulverized in a planetary mono mill (Fritsch, Germany (Pulverisette-7)).

Table 2 shows the properties of the bowl and balls used in the dry milling process. The milling condition is shown in Table 3. After milling, the frit size was analyzed by particle size analyzer (LS230 & N4PLUS, Coulter Corporation, USA). The elastic modulus and hardness of cullets were detected by nanoindentation (TriboIndenter, Hysitron Inc., USA). Melted glass was poured into a graphite mold for bulk glass and annealed at 10 °C over the glass transition temperature ( $T_g$ ). The density of the glass bulk was determined by Archimedes method.

### 3. Results and discussion

Fig. 1 shows the raw data of particle size distribution with A and B glasses. The particle size of A glass was smaller than that of B glass. Furthermore, A and B glasses were easily pulverized with increasing ball size, possibly due to the effect of the impact energy.<sup>3</sup> When the size of solids is gradually reduced with increasing energy consumption, their relation generally follows the formula,  $dD/dE_c = -k_1 D^q$ , where  $D$  is the particle diameter,  $E_c$  the energy input, and  $k_1$  and  $q$  are constants.<sup>7</sup> The equation was later converted by Rittinger<sup>8</sup> with the surface energy determined by the following equation:  $E_c = k'_r(1/D_p - 1/D_f) = k_r(S_p - S_f)$ , where  $S_p$  and  $S_f$  are the specific surface of product and feed, respectively, and  $k'_r$  and  $k_r$  are constants. This indicates that the input energy is consumed to increase the specific surface of the particles, i.e., increasing ball size and decreasing particle size are related to increased energy consumption.

In order to determine the relationship between mean particle size and ball size, the mean particle size of A and B glasses was plotted against increasing ball size, as shown in Fig. 2. The mean particle size of A and B glasses using 1mm milling balls differed by 13 μm, indicating that the comminution can be closely dependent upon the glass brittleness of A and B glasses in the milling condition. However, with milling balls larger than

1 mm, the reduction of the mean particle size could be slightly related to the glass brittleness but mostly to the impact energy. The difference between the mean particle size of the A and B glasses decreased from 13 to 3 μm as the ball size increased from 1 to 3 mm. Thus, if sufficient energy to produce a fine particle size of at least 0.4 μm is applied to the glass grinding, then the glass brittleness becomes independent of the mean particle size reduction.

In Fig. 3, the difference between the particle size of the A and B glasses in the particle size distribution increases for all

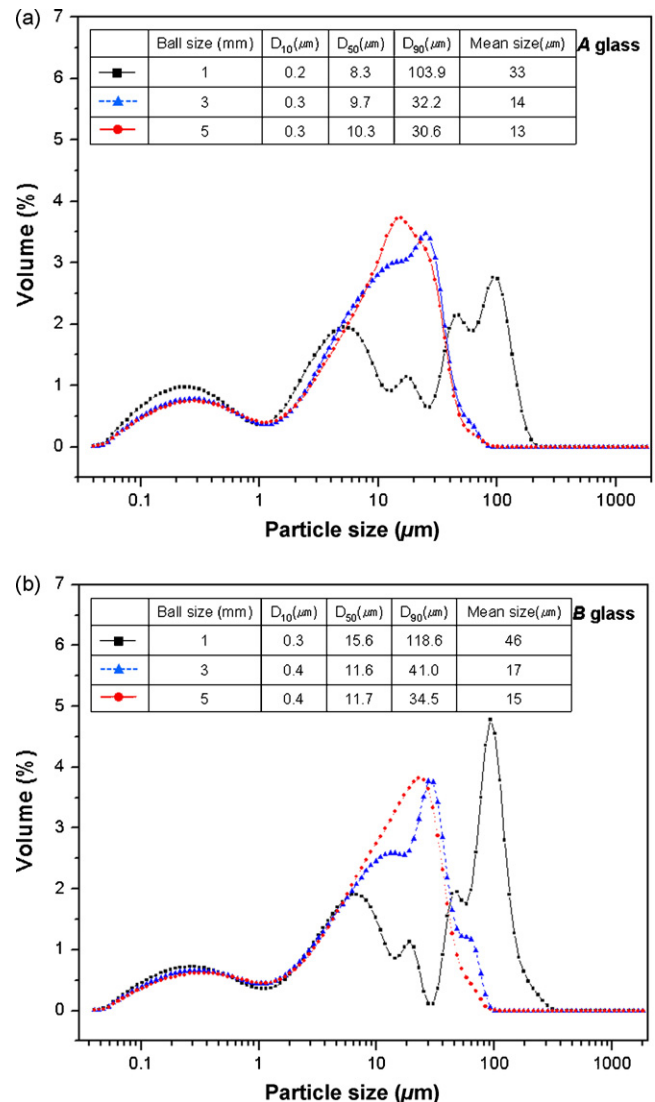


Fig. 1. Particle size distribution as a function of milling condition with A (a) and B (b) glasses for ball size of 1, 3 and 5 mm, respectively.

Table 2  
Properties of bowl and balls for the milling process

ZrO <sub>2</sub> (zirconia)	YTZ (balls)	PSZ (bowl)
Density (g/cm <sup>3</sup> )	>6.00	5.7
Color	White	Ivory
Micro hardness (MPa)	1150–1200	1500
Elastic modulus (GPa)	210–220	200
Modulus of rupture (MPa)	>1000	820
Fracture toughness (MPa m <sup>1/2</sup> )	12–14	8–12

Table 3  
Experimental condition of dry milling

Volume of bowl (cm <sup>3</sup> )	Contents of powder (g)	Contents of ball (g)	rpm	Ball shape	Ball size and weight (mm–mg)	Milling time (min/times)	Pausing time (min/times)
250	10	15	300	Spherical	1–1 3–87 5–413	10/6	10/5

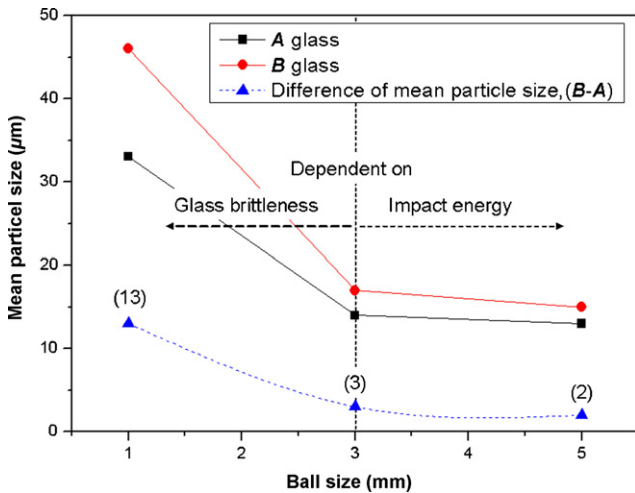


Fig. 2. Mean particle size of A and B glasses with the ball size.

ball sizes. The difference between the  $D_{10}$  particle size distribution of the A and B glasses was nearly zero for all ball sizes, indicating the absence of any effective size reduction because the brittleness and impact energy were inapplicable in the  $D_{10}$  particle size distribution. However, the difference between the particle size of the A and B glasses was significantly different in the  $D_{50-90}$  particle size distribution, indicating that the  $D_{50-90}$  of the A and B glasses is closely related to the brittleness. Furthermore, the difference of the mean particle size was decided with the  $D_{50-90}$ , rather than  $D_{10}$ , size distribution. Even if the mean particle size is equal among glasses with increasing ball size or

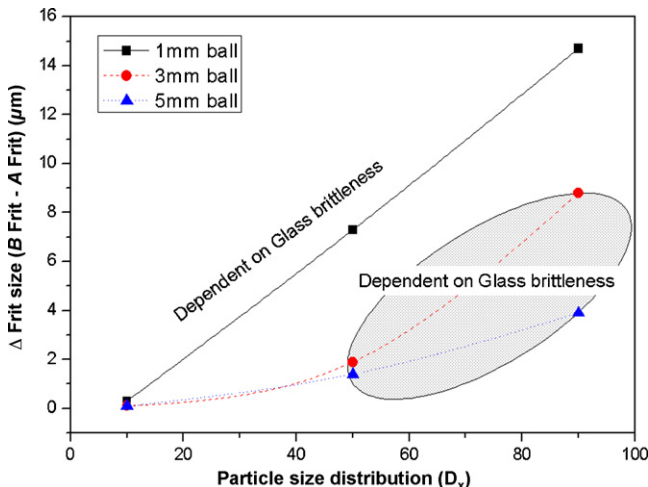


Fig. 3. Difference between the frit size distribution of A and B with the ball size.

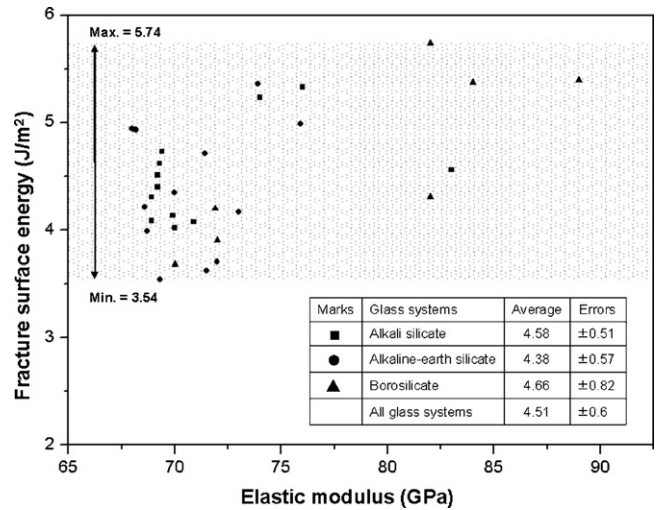


Fig. 4. Fracture surface energy of various glasses estimated from their elastic modulus.<sup>9–25</sup>

impact energy, the particle size differs in the particle size distribution. Therefore, the glass size reduction can only be decided by their brittleness in the particle size distribution.

Based on several studies,<sup>9–25</sup> we calculated the fracture surface energy with the fracture toughness and elastic modulus of glasses obtained from the literature values on the alkali silicate, alkali-earth silicate and borosilicate glass systems (Fig. 4). As shown in Fig. 4, the fracture surface energy of various glasses was approximately  $4.51 \pm 0.6 \text{ J/m}^2$ . To calculate the fracture surface energy of glasses, the fracture toughness ( $K_{IC}$ ) given by  $K_{IC} = (2\gamma_f E)^{1/2}$ , where  $\gamma_f$  and  $E$  are the fracture surface energy and elastic modulus, respectively, was used. In principle, the mechanism of glass size reduction is based on the fracture characteristics of a single particle and the frequency of each particle being crushed during pulverizing operations.<sup>4–8</sup> Lower fracture toughness allows easier pulverization.<sup>7,8</sup> Nucleation of cracks in frits is supposed to be derived from thermal shock or thermal stress during quenching to produce cullet from molten glass. Assuming that the crack initiation, such as the crack source, and the distribution of cracks in frits are equal in three glasses (A, B, L) because of the same frit preparation condition, the crack propagation for splitting frits can follow the Griffith equation.<sup>29</sup> Only the energy necessary to create two new surfaces at the tip of the crack is required for crack propagation.

Based on the fracture surface energy, we assumed that in any glass systems the glass fracture toughness can be calculated using the elastic modulus. When the average of the fracture surface energy ( $4.51 \pm 0.6 \text{ J/m}^2$ ) was considered with the experi-

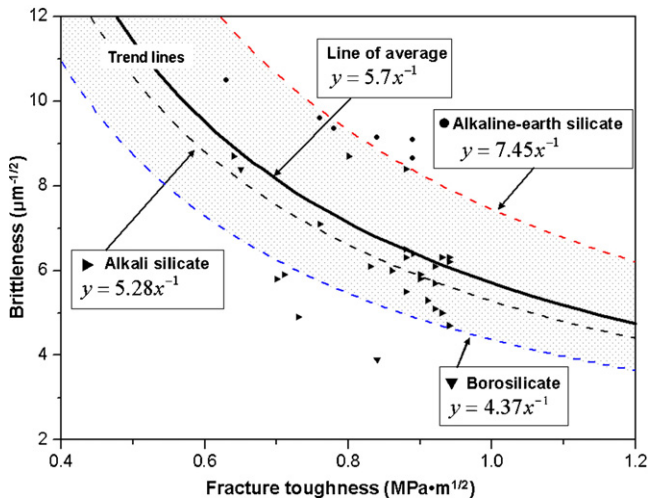


Fig. 5. Brittleness of various glasses estimated from their fracture toughness.<sup>6,26</sup>

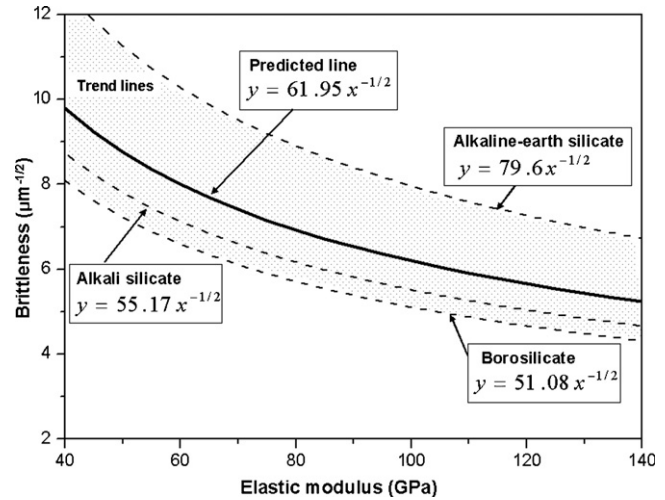


Fig. 6. Estimation of brittleness from the elastic modulus of glasses.

mental data of elastic modulus for L glass, the fracture toughness ranged from 0.73 to 0.83 ( $\text{MPa m}^{1/2}$ ). The average of the fracture toughness for L glass was about 0.78 with an error of  $\pm 0.03$ . The same method produced fracture toughness values of A and B glasses of about  $0.85 \pm 0.03$  and  $0.91 \pm 0.04 \text{ MPa m}^{1/2}$ , respectively.

Furthermore, the fracture toughness is related to the brittleness, as shown in Fig. 5.<sup>6,26</sup> The brittleness of the various glasses ranged from 4 to  $11 \mu\text{m}^{-1/2}$  and the fracture toughness from 0.6 to  $1 \text{ MPa m}^{1/2}$ . The brittleness ( $B$ ) of the glasses is described by the ratio of Vickers hardness/fracture toughness:  $B = H_v/K_{IC}$ .<sup>27,28</sup> This equation for the relationship between brittleness and fracture toughness is governed by the Vickers hardness shown in Fig. 5. On the other hand, the brittleness is reported to be related to the density with two types of glass systems, silicate and borate glass, which have a low density ( $1.8\text{--}2.8 \text{ g/cm}^3$ ).<sup>6</sup> However, at  $4.7\text{--}5.4 \text{ g/cm}^3$  the density of our experimental glasses was outside of this density range. In different glass systems having similar density, brittleness could be dependent on other physical factors.

The brittleness of the glasses was calculated by the experimental hardness and fracture toughness of L, A and B glasses predicted by the average of the fracture surface energy in various glasses (Table 4). Comparing the similarly dense L and A glasses, the brittleness of L glass was higher than that of A glass which had a higher elastic modulus. However, the brittleness of

A glass was similar to that of B glass, although they were the same glass family. This result may have been caused by other properties such as density, elastic modulus, and hardness, and to experimental error.

We suggest other methods for predicting the glass brittleness. First, the brittleness is predicted by the relationship between brittleness and fracture toughness, as determined from Fig. 5. We calculated the equations with the fracture toughness of the experimental glasses, which were predicted by the average of the fracture surface energy in various glasses. Secondly, the expression,  $B = H_v/(2\gamma_f E)^{1/2} = \delta(E)^{-1/2}$  can be obtained by rearranging the brittleness,  $B = H_v(\text{hardness})/K_{IC}$ , which is itself given by the relationship between the brittleness and elastic modulus of the same glass family (alkaline-earth silicate, alkali silicate, and borosilicate) as measured by the fracture surface energy and the Vickers hardness in various glasses, as shown in Figs. 4 and 5. By the second method, the brittleness of various glass systems is plotted against the elastic modulus of the glasses, as shown in Fig. 6. The brittleness in the region between the boundaries of alkaline-earth silicate and borosilicate is correlated to the elastic modulus of the glasses.

Table 4 presents the density, elastic modulus and hardness of the three glasses (L, A and B), along with their fracture toughness and brittleness as predicted by several empirical equations. The brittleness of our experimentally produced glasses were predicted to be about  $7.51 \mu\text{m}^{-1/2}$  for lead glass (L) having an elastic modulus of 68 GPa, and  $6.93$  and  $6.46 \mu\text{m}^{-1/2}$  for bis-

Table 4  
Density, elastic modulus, and hardness, and predicted fracture toughness and brittleness of the three glasses

Samples	Density ( $\text{g/cm}^3$ )	Elastic modulus (GPa)	Hardness (GPa)	$K_{IC}^a$ ( $\text{MPa m}^{1/2}$ )	Brittleness <sup>b</sup> ( $\mu\text{m}^{-1/2}$ )	Brittleness <sup>c</sup> ( $\mu\text{m}^{-1/2}$ )	Brittleness <sup>d</sup> ( $\mu\text{m}^{-1/2}$ )
L	4.8	68	5.34	$0.78 \pm 0.03$	$7.37 \pm 0.62$	$7.31 \pm 2.02$	$7.51 \pm 1.87$
A	4.7	80	5.94	$0.85 \pm 0.03$	$7.55 \pm 0.63$	$6.71 \pm 1.86$	$6.93 \pm 1.72$
B	5.4	92	6.36	$0.91 \pm 0.04$	$7.54 \pm 0.63$	$6.26 \pm 1.74$	$6.46 \pm 1.61$

<sup>a</sup> Predicted by Fig. 4.

<sup>b</sup> Calculated by the  $H_v/K_{IC}$  ratio.<sup>27–28</sup>

<sup>c</sup> Predicted by  $K_{IC}$  and Fig. 5.

<sup>d</sup> Predicted by Fig. 6.

mate glass (A and B) having an elastic modulus of 80 and 92 GPa, respectively.

#### 4. Conclusion

We examined the relationship between particle size distribution and glass brittleness for different frits. The particle size distribution ( $D_{50-90}$ ) of glasses was dependent upon their brittleness in dry milling process. The mechanical properties of the lead glass were significantly lower than those of the lead-free glasses. Thus, the size reduction of the glass frits was significantly related to the mechanical properties with the  $D_{50-90}$  particle size distribution. Especially, the brittleness of the glasses was closely related to the  $D_{50-90}$  particle size distribution and the size reduction. Finally, the glass brittleness could be predicted with the elastic modulus for efficient pulverization.

#### Acknowledgements

This work is financially supported by the Ministry of Education and Human Resources Development (MOE), the Ministry of Commerce, Industry and Energy (MOCIE) and the Ministry of Labor (MOLAB) through the fostering project of the Lab of Excellency.

#### References

- Kim, D. N., Lee, J. Y., Huh, J. S. and Kim, H. S., Thermal and electrical properties of BaO–B<sub>2</sub>O<sub>3</sub>–ZnO glasses. *J. Non-Cryst. Solids*, 2002, **306**, 70–75.
- Cha, M. R., Hwang, S. J. and Kim, H. S., Formation of layer on bismate frit surface during wet milling. *Mater. Sci. Forum*, 2006, **510–511**, 582–585.
- Hwang, S. J., Kim, Y. J., Shim, S. B. and Kim, H. S., Chemical durability of frits used in process of plasma display panels. *Solid State Phenomena*, 2007, **124–126**, 435–438.
- Kano, J., Mio, H. and Saito, F., Correlation of size reduction rate of inorganic materials with impact energy of balls in planetary ball milling. *J. Chem. Eng. Jpn.*, 1999, **32**, 445–448.
- Okada, K., Kikuchi, S., Ban, T. and Otsuka, N., Difference of mechanochemical factors for Al<sub>2</sub>O<sub>3</sub> powders upon dry and wet grinding. *J. Mater. Sci. Lett.*, 1992, **11**, 862–864.
- Sehgal, J. and Ito, S., Brittleness of glass. *J. Non-Cryst. Solids*, 1999, **253**, 126–132.
- Walker, W. H., Lewis, W. K., McAdams, W. H. and Gilliland, E. R., *Principles of Chemical Engineering (3rd ed.)*. McGraw-Hill, New York, 1937.
- Koichi, L., Keishi, G. and Ko, H., *Powder Technology Handbook (1st ed.)*. Marcel Dekker Inc., New York, 1991.
- Yoshida, S., Tanaka, H., Hayashi, T., Matsuoka, J. and Soga, N., Scratch resistance of sodium borosilicate glass. *J. Ceram. Soc. Jpn.*, 2001, **109**, 511–515.
- Watanabe, T., Muratsubaki, K., Benino, Y., Saitoh, H. and Komatsu, T., Hardness elastic properties of Bi<sub>2</sub>O<sub>3</sub>-based glasses. *J. Mater. Sci.*, 2001, **35**, 2427–2433.
- Baikova, L. G., Fedorov, Y. K., Pukh, V. P., Tikhonova, L. V., Kazannikova, T. P., Sinani, A. B. and Nikitina, S. I., The influence of silicon oxide on the mechanical properties of metaphosphate glasses. *Glass Phys. Chem.*, 2004, **30**, 420–424.
- Nagae, T., Kitahara, H., Ikeda, K., Yoshida, F., Nakashima, H., Ito, S. and Abe, H., Evaluation of indentation induced residual stress on the surface of substrate glasses for display. *J. Ceram. Soc. Jpn.*, 2002, **110**, 834.
- Bertoldi, M. and Sglavo, V. M., Influence of composition on fatigue behavior and threshold stress inquiry factor of borosilicate glasses. *J. Am. Ceram. Soc.*, 2002, **85**, 2499–2506.
- Deriano, S., Rouxel, T., Lefloch, M. and Beuneu, B., Structure and mechanical properties of alkali-alkaline earth-silicate glasses. *Phys. Chem. Glasses*, 2004, **45**, 37–44.
- Yoshida, S., Hidaka, A. and Matsuoka, J., Crack initiation behavior of sodium aluminosilicate glasses. *J. Non-Cryst. Solids*, 2004, **344**, 37–43.
- Deriano, S., Jarry, A., Rouxel, T., Sangleboeuf, J. C. and Hampshire, S., The indentation fracture toughness ( $K_{IC}$ ) and its parameters: the case of silica-rich glasses. *J. Non-Cryst. Solids*, 2004, **344**, 44–50.
- LeHouerou, V., Sangleboeuf, J. C., Deriano, S., Rouxel, T. and Duisit, G., Surface damage of soda–lime–silica glasses: indentation scratch behavior. *J. Non-Cryst. Solids*, 2003, **316**, 54–63.
- LeBourhis, E. and Rpxel, T., Indentation response of glass with temperature. *J. Non-Cryst. Solids*, 2004, **316**, 153–159.
- Seal, A., Dalui, S. K., Mukhopadhyay, A. K., Phani, K. K. and Maiti, H. S., Mechanical behavior of glass polymer multilayer composites. *J. Mater. Sci.*, 2003, **38**, 1063.
- Deriano, S., Rouxel, T., LeFloch, M. and Beuneu, B., Structure mechanical properties of alkali-alkaline earth-silicate glasses. *Phys. Chem. Glasses*, 2004, **45**, 37–44.
- Romero, M., Rawlings, R. D. and Rincón, J. M., Crystal nucleation and growth in glasses from inorganic wastes from urban incineration. *J. Non-Cryst. Solids*, 2000, **271**, 106–118.
- Donald, I. W., Metcalfe, B. L. and Taylor, J. R. N., The immobilization of high level radioactive wastes using ceramics and glasses. *J. Mater. Sci.*, 1997, **32**, 5851–5887.
- Gehrke, E., Hähnert, M. and Ullner, C., Influence of dissolution rate on crack growth and fatigue of Na<sub>2</sub>O–Al<sub>2</sub>O<sub>3</sub>–B<sub>2</sub>O<sub>3</sub> SiO<sub>2</sub> glasses. *J. Mater. Sci.*, 1987, **22**, 1682–1686.
- Siadati, M. H., Chawla, K. K. and Ferber, M., The role of the SnO<sub>2</sub> interphase in an alumina/glass composite: a fractographic study. *J. Mater. Sci.*, 1991, **26**, 2741–2749.
- Yoshimoto, M. and Soga, N., Improvement of mechanical properties of metaphosphate glass by addition of chromium oxide. *Chem. Lett.*, 1987, 1711–1714.
- Rouxel, T., Dely, N., Sangleboeuf, J. C., Deriano, S., LeFloch, M., Beuneu, B. and Hampshire, S., Structure–property correlations in Y–Ca–Mg–sialon glasses: physical and mechanical properties. *J. Am. Ceram. Soc.*, 2005, **88**(4), 889–896.
- Lawn, B. R. and Marshall, D. B., Hardness, toughness and brittleness: an indentation analysis. *J. Am. Ceram. Soc.*, 1979, **62**(7–8), 347–350.
- Quinn, J. B. and Quinn, G. D., Indentation brittleness of ceramics: a fresh approach. *J. Mater. Sci.*, 1997, **32**, 4331–4346.
- Nevill mott, F. R. S. and Noakes, G. R., *The Physical Properties of Glass*. Wykeham Publications, London, 1973.